7th ECCOMAS Thematic Conference on Smart Structures and Materials
SMART 2015
A.L. Araúo, C.A. Mota Soares, et al. (Editors)

SPATIAL COMPATIBILITY FILTERS FOR STRUCTURAL HEALTH MONITORING

Markus Zellhofer* & **Michael Krommer†**

* Linz Center of Mechatronics
Altenbergerstrasse 69, A-4040 Linz, Austria
e-mail: markus.zellhofer@lcm.at

† Institute of Mechanics and Mechatronics, Vienna University of Technology
Getreidemarkt 9, A-1060 Vienna, Austria
e-mail: michael.krommer@tuwien.ac.at

Keywords: Structural Health Monitoring, Spatial filters, Incompatible strains, Compatibility filters.

Summary: *Spatial filters are spatially distributed sensors, which filter a specific content of the deformation or vibration of a structure. Typically, they are put into practice by sensors, which are sensitive to the strain in a deformed structure. The most commonly used type is a modal filter, which filters one specific vibration mode of a structure. Applications of modal filters are in the field of vibration control as well as in Structural Health Monitoring. In the latter context the frequency response function obtained from the modal filter has only a single peak, if the structure is undamaged. If damage occurs, additional peaks appear in the frequency response function, from which one can conclude on the presence of damage. Besides the fact, that using modal filters for Structural Health Monitoring enables damage detection only indirectly, it is also a method, for which detailed information concerning the structure is needed; in particular, the constitutive relations are crucial for the computation of the vibration modes, which are needed to design the modal filters. In the present paper we propose a different type of spatial filter for Structural Health Monitoring - Spatial Compatibility Filters. Such filters filter the incompatible part of the strain tensor; hence, their signal is trivial, if the strain tensor is comaptible. A non-trivial signal results only from the presence of incompatible parts of the strain tensor, which is the case for damaged structures. Hence, the signal of a compatibility filter can be directly related to damage. Moreover, the design of the filter only requires geometrical information about the structure, but no constitutive relations. Based on the concept of compatibility filters, we discuss their use for different levels of Structural Health Monitoring: Damage detection, localisation and quantification.*

1. Introduction

A spatial filter is a sensor, which filters certain spatial information; e.g. modal filters, which filter the modal content of only one vibration mode (Lee and Moon [1]), displacement filters,

which filter the displacement of a specific point in a specific direction (Krommer and Irschik [2]) or volume displacement filters (see Preumont et.al. [3]). Such spatial filters are widely used in structural control (e.g. Preumont et.al. [4]) and structural health monitoring (e.g. Deraemaeker and Preumont [5]). It has been mentioned in the literature that spatial filters can be put into practice either by continuously distributed sensors or by arrays of dense sensors. In the present paper we consider the first case only, in which the signal of a spatial filter represents a weighted integral of the strain a body is suffering; such continuously distributed sensors may be implemented using piezoelectric materials or optical fibers. Concerning the use of piezoelectric sensors in structural mechanics we refer to Irschik et.al. [6].

In the present paper we study an alternative type of spatial filters; namely compatibility filters, which filter the incompatible part of the strain tensor by a proper choice of the weights in the definition of the signal of a spatial filter. In earlier works such filters have also been denoted as *nilpotent* sensors, see Irschik et.al [7]. We consider compatibility filters, which we will introduce in this paper, as a novel and innovative concept for damage detection, localisation and quantification. The general idea of detecting defects and damage from the incompatibility of the strain tensor has been suggested by Wildy et.al. [8]. However, in the latter paper this idea has not been combined with spatial filtering. In general, it is accepted that the micromechanics of defects and damage is strongly related to the concept of incompatible strains; or in other words *eigenstrains*, see Mura [9]; e.g. it applies to problems concerned with inclusions, cracks, dislocations, etc.

2. Governing equations

We study the three-dimensional problem of a material body with volume V, a sketch of which is shown in Fig. 1. The boundary ∂V is composed of two parts. On the part ∂V_u homoge-

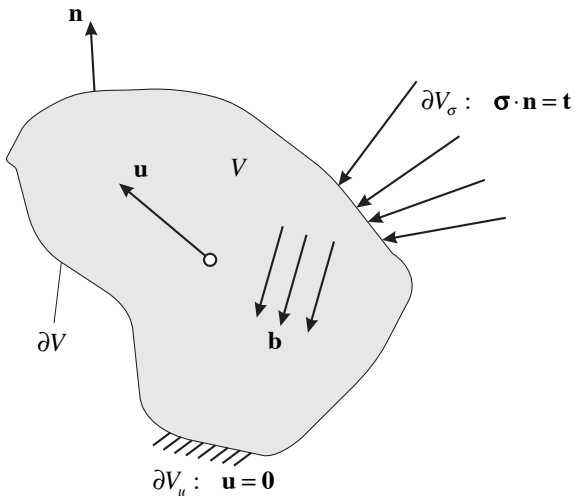

Figure 1. Three-dimensional material body with surface tractions and body forces

nous kinematical boundary conditions are prescribed, whereas at ∂V_σ tractions $\mathbf{t}$ act; within V

body forces $\mathbf{b}$ are applied. The balance equations and the boundary conditions are

$$\begin{aligned} V: &\quad \nabla \cdot \boldsymbol{\sigma}(\mathbf{r},t) + \mathbf{b}(\mathbf{r},t) = \rho \ddot{\mathbf{u}}(\mathbf{r},t), \\ \partial V_\sigma: &\quad \boldsymbol{\sigma}(\mathbf{r},t) \cdot \mathbf{n} = \mathbf{t}, \\ \partial V_u: &\quad \mathbf{u}(\mathbf{r},t) = \mathbf{0}. \end{aligned} \tag{1}$$

Here, $\boldsymbol{\sigma}$ is the symmetric stress tensor and $\mathbf{n}$ the unit normal vector of the boundary pointing outwards; $\mathbf{r}$ is the position vector of an arbitrary point P. Moreover, $\mathbf{u}$ is the displacement vector and ρ the mass density.

3. Spatial filters

A spatial filter is a distributed sensor, whose signal is

$$y(t) = \int_V \mathbf{S}(\mathbf{r}) \cdot\cdot\, \boldsymbol{\varepsilon}(\mathbf{r},t) dV. \tag{2}$$

$\boldsymbol{\varepsilon}(\mathbf{r},t)$ is the strain tensor and the tensor $\mathbf{S}(\mathbf{r})$ is the so-called shape tensor. The general goal of sensor design is to choose the latter, such that the signal has a meaningful mechanical interpretation. In order to enable a simple design, we introduce an auxiliary quasi-static problem with the same geometry as the original problem and with identical kinematical boundary conditions at ∂V_u; see Fig. 2 for the auxiliary problem. We apply static external body forces $\mathbf{b}^{(aux)}$ and

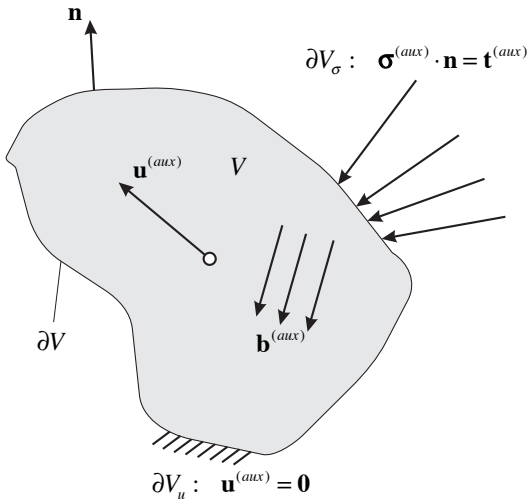

Figure 2. Three-dimensional quasi-static auxiliary problem

static external tractions $\mathbf{t}^{(aux)}$ at that part of the boundary, at which tractions are applied in the original problem; namely, ∂V_σ. Then, the principle of virtual work for the auxiliary problem reads

$$\int_V \boldsymbol{\sigma}^{(aux)} \cdot\cdot\, \delta\boldsymbol{\varepsilon} dV = \int_V \mathbf{b}^{(aux)} \cdot\, \delta\mathbf{u} dV + \int_{\partial V_\sigma} \mathbf{t}^{(aux)} \cdot\, \delta\mathbf{u} dS. \tag{3}$$

Here, $\boldsymbol{\sigma}^{(aux)}$ is a statically admissible stress tensor (see e.g. Gurtin [12] for a definition), which must satisfy

$$\begin{aligned} V: \quad & \nabla \cdot \boldsymbol{\sigma}^{(aux)}(\mathbf{r}) + \mathbf{b}^{(aux)}(\mathbf{r}) = \mathbf{0}, \\ \partial V_\sigma: \quad & \boldsymbol{\sigma}^{(aux)}(\mathbf{r}) \cdot \mathbf{n} = \mathbf{t}^{(aux)}(\mathbf{r}), \end{aligned} \tag{4}$$

and which in general is not unique. We use the displacement vector $\mathbf{u}(\mathbf{r}, t)$ and the strain tensor $\boldsymbol{\varepsilon}(\mathbf{r}, t)$ of the original problem as the virtual displacement vector $\delta\mathbf{u}$ and the virtual strain tensor $\delta\boldsymbol{\varepsilon}$ in Eq. (3) and we choose the shape tensor as any statically admissible stress tensor in the auxiliary problem, $\mathbf{S}(\mathbf{r}) = \boldsymbol{\sigma}^{(aux)}(\mathbf{r})$. Then, the signal of a spatial filter is

$$y(t) = \int_V \mathbf{b}^{(aux)}(\mathbf{r}) \cdot \mathbf{u}(\mathbf{r}, t) dV + \int_{\partial V_\sigma} \mathbf{t}^{(aux)}(\mathbf{r}) \cdot \mathbf{u}(\mathbf{r}, t) dS. \tag{5}$$

Hence, a proper choice of the forces in the auxiliary problem finds a sensor, the signal of which is the work conjugate to the auxiliary forces. An overview discussing different choices of these auxiliary forces has been given by Krommer and Irschik [2].

A classical example for such a spatial filter is a modal filter, which was introduced by Lee and Moon in [1], and which filters the modal content of one vibration mode only. Modal filters are very well known types of spatial filters and are widely used in vibration control (e.g. [4]), but also in the context of structural health monitoring, as introduced by Deraemaeker and Preumont [5]. In the present paper we will be using a related type of a spatial filter for structural health monitoring, namely compatibility filters; in particular, for damage detection, localisation and quantification. The latter concept of compatibility filters represents a novel concept in the field of structural health monitoring.

4. Compatibility filters

We introduce the idea of a compatibility filter as a special case of a spatial filter, which has a trivial signal

$$y(t) = \int_V \mathbf{S}(\mathbf{r}) \cdot\cdot \boldsymbol{\varepsilon}(\mathbf{r}, t) dV = 0 \tag{6}$$

in case the strain tensor is compatible. From Eq. (5) we find that Eq. (6) holds, if the external forces in the auxiliary problem are zero, $\mathbf{b}^{(aux)}(\mathbf{r}) = \mathbf{0}$ and $\mathbf{t}^{(aux)}(\mathbf{r}) = \mathbf{0}$; hence, the shape tensor can be computed from

$$\begin{aligned} V: \quad & \nabla \cdot \mathbf{S}(\mathbf{r}) = \mathbf{0}, \\ \partial V_\sigma: \quad & \mathbf{S}(\mathbf{r}) \cdot \mathbf{n} = \mathbf{0}. \end{aligned} \tag{7}$$

We note again that the shape tensor $\mathbf{S}(\mathbf{r})$ represents a statically admissible stress tensor, which is not unique in case the problem is not statically determinate and not trivial even for the case the external forces in the auxiliary problem are zero. A shape tensor that satisfies Eq. (7) is denoted as a nilpotent shape tensor. The idea of nilpotent sensors has been studied in detail

by Irschik et.al. [7], in which it is mentioned that such sensors are inappropriate for measuring structural entities (e.g. displacements or slopes) as their signal is trivial. Since then applications for optimizing sensor distributions by a proper superposition of nilpotent sensors have been discussed, see e.g. Krommer et.al. [10], and the use for damage detection in simple beam structures has been introduced in Krommer and Zellhofer [11]. In the present paper we put this novel concept for damage detection into a more theoretical framework by identifying nilpotent sensors as compatibility filters.

For that sake we proof that, if Eqs. (6) and (7) hold, $\boldsymbol{\varepsilon}$ must be compatible; hence, Eq. (6) represents a compatibility filter. First, we note that $\nabla \cdot \mathbf{S} = \mathbf{0}$ is identically satisfied, if

$$\mathbf{S} = \nabla \times (\nabla \times \boldsymbol{\Phi})^T \tag{8}$$

holds. $\boldsymbol{\Phi}$ is an arbitrary symmetric second rank tensor and denoted as a Beltrami stress tensor in the literature, see e.g. Gurtin [12]. In practical problems, for which $\mathbf{S} \cdot \mathbf{n} = \mathbf{0}$ must hold at ∂V_σ as well, $\boldsymbol{\Phi}$ must satisfy certain conditions at ∂V_σ, which we do not wish to discuss here. As another pre-requisite, we note the general compatibility conditions

$$\mathbf{R} = \nabla \times (\nabla \times \boldsymbol{\varepsilon})^T = \mathbf{0}. \tag{9}$$

We can now write the signal of a compatibility filter as

$$y(t) = \int_V \mathbf{S} \cdot\cdot \boldsymbol{\varepsilon} dV = \int_V \nabla \times (\nabla \times \boldsymbol{\Phi})^T \cdot\cdot \boldsymbol{\varepsilon} dV. \tag{10}$$

Next, we apply integral transforms to the integral and assume that the tensors $\boldsymbol{\Phi}$ and $\boldsymbol{\varepsilon}$ satisfy certain conditions at the boundary, which follow from the kinematical and dynamical boundary conditions and which ensure no boundary integrals are non trivial. This results into

$$y(t) = \int_V \boldsymbol{\Phi} \cdot\cdot \mathbf{R} dV. \tag{11}$$

Note that the boundary integrals my not be zero, if certain compatbility conditions at the boundary are not satisfied; nonetheles, this case also relates to the notion of a compatibility filter, if it is not only understood locally within the volume V, but also with respect to the boundary. In general, we conclude that the signal of a compatibility filter is trivial, if the incompatibility tensor $\mathbf{R} = \nabla \times (\nabla \times \boldsymbol{\varepsilon})^T$ vanishes; it is not trivial, if incompatibility is present.

This is indded the case for many practical problems; e.g. for the case the displacement vector experiences a discontinuity at some internal surface of the material body. In the following this case will be discussed in some detail.

5. Discontinuous displacements

As a specific type of incompatibility, we consdier discontinuous displacements. If the displacement vector $\mathbf{u}(\mathbf{r}, t)$ in our original problem experiences a discontinuity $[\![\mathbf{u}]\!] \neq \mathbf{0}$ at an

internal surface of the body under consideration, say S_{12}, it is clear that the strain tensor does no longer satisfy the compatibility conditions. Moreover, the displacement field is not kinematically admissible for the quasi-static auxiliary problem previously used in the principle of virtual work. To ensure the latter kinematical admissibility, we introduce a different auxiliary problem, for which certain kinematical constraints at S_{12} are released, such that the displacement field of the original problem becomes admissible for the auxiliary problem. For a sketch of this auxiliary problem see Fig. 3. Body forces in V and surface tractions at ∂V_σ are absent;

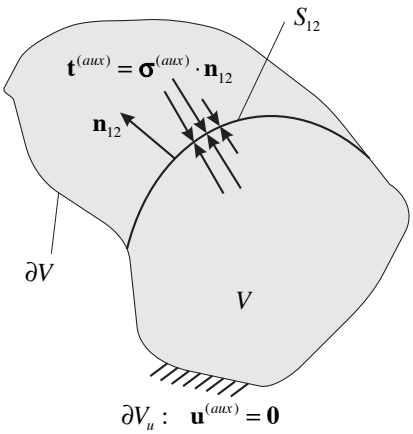

Figure 3. Three-dimensional quasi-static auxiliary problem with discontinuity surface

at S_{12} tractions $\mathbf{t}^{(aux)}$ are applied at both sides of the discontinuity surface, which are identical but of opposite sign. At the surface with unit outer normal vector $\mathbf{n}_{12}$ these tractions are computed from $\mathbf{t}^{(aux)} = \boldsymbol{\sigma}^{(aux)} \cdot \mathbf{n}_{12}$, where $\boldsymbol{\sigma}^{(aux)}$ is any statically admissible stress tensor for the original auxiliary problem without body forces and surface tractions; hence, from nilpotent shape tensors as defined in Eq. (7), $\mathbf{S} = \boldsymbol{\sigma}^{(aux)}$. It then follows from Eq. (5) that the signal of a compatibility filter becomes

$$y(t) = \int_V \mathbf{S}(\mathbf{r}) \cdot\cdot \boldsymbol{\varepsilon}(\mathbf{r}, t) dV = -\int_{S_{12}} (\mathbf{S} \cdot \mathbf{n}_{12}) \cdot [\![\mathbf{u}]\!] \, dS; \tag{12}$$

hence, the signal is a weighted average over the jump the displacement vector experiences at the discontinuity surface S_{12}. This latter fact can be utilized to detect displacement discontinuities using compatibility filters. Moreover, nilpotent shape tensors also exist for the case the tractions $\mathbf{t}^{(aux)}$ at S_{12} are zero; this fact can be used to localize damage, which in the case of discontinuities means the location of the internal surface. With respect to discontinuous displacements related to damage, we mention two examples.

1. The theory of plasticity, in which the tangential components of the displacement vector are sometimes assumed to be discontinuous across an internal surface; the normal component of the displacement vector in contrast must be continuous, see Prager and Hodge [13].

2. The field of crack mechanics, for which the so-called *Crack Opening Displacement*, which is a displacement discontinuity, is of particular importance, as it can be related to stress intensity factors, see e.g. Mura [9].

5.1 A simple example with discontinuous displacements

As a simple example we consider a straight beam of length L under the assumption of plane bending using the Bernouli-Euler kinematic hypothesis. The notion of shape tensors then refers to the notion shape functions $S(x)$. In particular, nilpotent shape functions are computed as bending moments for the beam without any force loading,

$$\frac{\partial^2 S(x)}{\partial x^2} = 0, \tag{13}$$

for which $S(x)$ has to satisfy homogenous dynamical boundary conditions, if dynamical boundary conditions are prescribed in the actual beam. The number of nilpotent shape functions is identical to the grade of redanduncy of the beam. E.g. two nilpotent shape functions exist for a one span beam that is clamped at both ends and whose grade of redundancy is 2; see Fig. 4. In

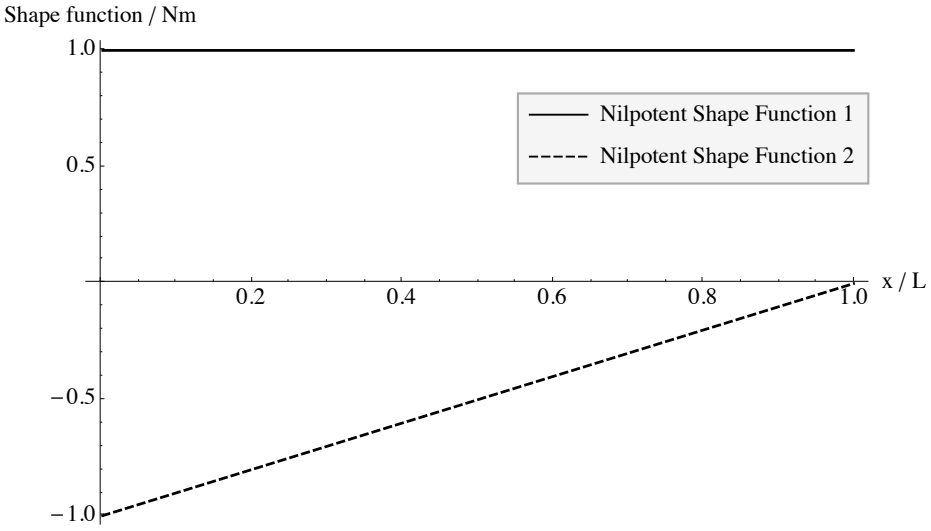

Figure 4. Nilpotent shape functions of a beam clamped at both ends

order to simulate the dynamics of this simple beam we take the bending stiffniss as $D = 1\text{Nm}^2$ and the linear inertia as $P = 1\text{kgm}^{-1}$. A span wise constant transverse force $p_0 = 1\text{Nm}^{-1}$ is applied harmonically and the response in the frequency domain is computed. In Fig. 5 the dynamic magnification factor is shown for the deflection at $x = L/2$ and for the two sensor signals resulting from compatibility filters put into practice by means of the two nilpotent shape functions shown in Fig. 4. One can see that the deflection is not zero; yet, the signals are trivial, because nilpotent sensors do not result into a signal in case the strain is compatible. In terms of the beam theory, compatibility refers to the continuity of the deflection and the slope as well

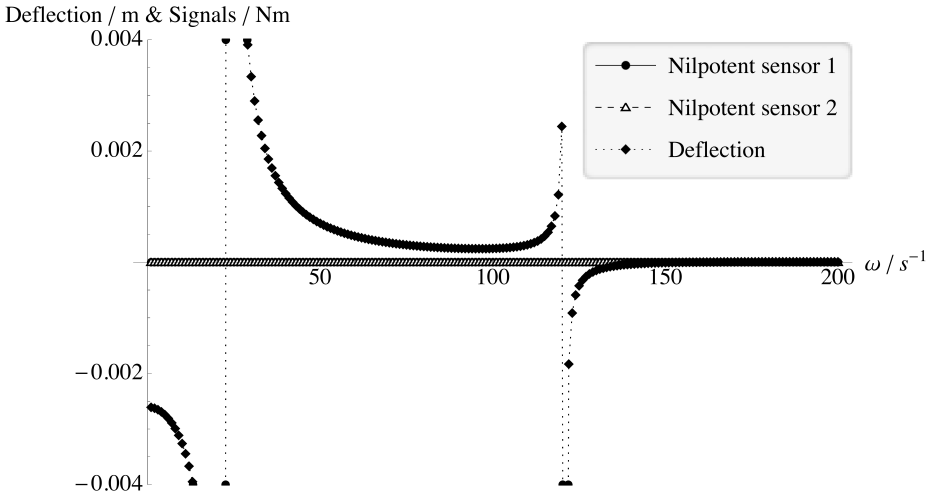

Figure 5. Nilpotent sensor signals & deflection

as to the kinematic boundary conditions. In the following, we will introduce incompatibility in terms of a kink; hence, in terms of a discontinuity of the slope, which occurs at an intermediate hinge.

We use this damage scenario of the intermediate hinge with a residual stiffness, because the effect of a crack on the stiffness of a beam can be approximated by a reduction of the stiffness in the vicinity of the crack. A fully local formulation models this stiffness reduction as an intermediate hinge with a rotational spring; the residual spring stiffness K is related to the crack depth d characterized by the non-dimensional ratio $\beta = d/t$ (with t the thickness of the rectangular cross section of the beam, which in our case is $t = L/100$) by means of

$$K = \frac{D}{t}\frac{1}{C(\beta)}, \tag{14}$$

with the nominal bending stiffness D of the beam cross section. Different methods to compute the local compliance $C(\beta)$ have been reported in the literature; we use the one proposed in [14],

$$C(\beta) = 6\pi\beta^2(0.6384 - 1.035\beta + 3.7201\beta^2 - 5.1773\beta^3 + 7.553\beta^4 - 7.332\beta^5 + 2.4909\beta^6). \tag{15}$$

With respect to our example problem, we introduce a hinge at the location $x = L/3$ with a residual stiffness $K = 383.684$, which corresponds to a relative crack depth $\beta = 0.1$. Again, we apply a span wise constant transverse force loading harmonically. In Fig. 6 we present the dynamic magnification factor for the resulting kink at the location of the hinge at $x = L/3$ and for the two sensor signals resulting from compatibility filters put into practice by means of the two nilpotent shape functions. We see that in contrast to the undamged beam the signals from the nilpotent sensors are not trivial. Moreover, the signal from the first nilpotent sensor is identical to the resulting kink and the signal from the second nilpotent sensor is similar to the one from the first nilpotent sensor in the sense that it only differs by a constant factor. We now use the information from the two nilpotent sensors to detect, localize and quantify the damage.

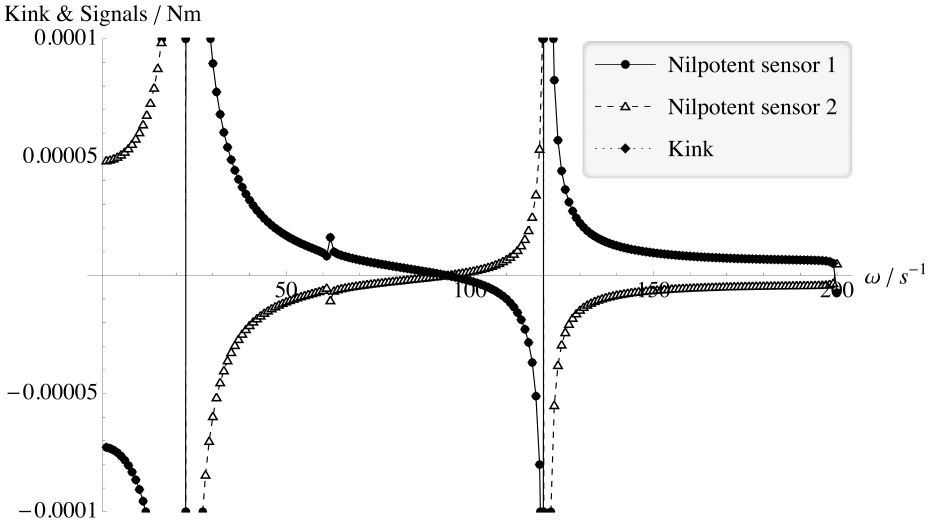

Figure 6. Nilpotent sensor signals & kink

5.1.1 Damage detection

Damage is detected simply by the fact that the nilpotent sensors have no trivial signal for the damaged case. In order to introduce damage indices, we introduce inner products of the signals. We use the sensor signals, which depend on the excitation frequency, $y_i = y_i(\omega)$, with $i = 1, 2$ to compute the components of a square matrix $\mathbf{A}$ as

$$A_{ij} = \int_0^{\bar{\omega}} y_i(\omega) y_j(\omega) d\omega \ , \quad i, j = 1, 2. \tag{16}$$

$\bar{\omega}$ is an upper bound of the excitation frequency used in the simulation. Then we define two damage indices D_i, with $i = 1, 2$ as

$$D_i = \frac{A_{ii}}{A_{ii,nominal}}. \tag{17}$$

Here, $A_{ii,nominal}$ are corresponding nominal values for the case of a small damage, which serve as reference values. In our example, we use a relative crack depth of $\beta_{nominal} = 0.01$ and we compute the two damage indices as

$$D_1 = D_2 = 148.944, \tag{18}$$

from which we conclude on the presence of damage in the beam.

5.1.2 Damage localization

As we have already mentioned, the signals from the two nilpotent sensors are identical besides a constant factor; hence, the rank of the matrix $\mathbf{A}$ is only 1 and one can compute a 1-dimensional null space. Rather then computing the null space, we solve the eigenvalue problem

for the matrix $\mathbf{A}$, from which we find one zero eigenvalue and one non zero eigenvalue. We use the matrix of the eigenvectors

$$\mathbf{T} = \left[\mathbf{e}_1^T \ \mathbf{e}_0^T\right] \tag{19}$$

as a transformation matrix. Here, $\mathbf{e}_0$ is the eigenvector for the zero eigenvalue and $\mathbf{e}_1$ the eigenvector for the non zero eigenvalue. The transformation is applied to the nilpotent shape functions $S_i(x)$. With the aid of this transformation we obtain adjusted nilpotent shape functions $\bar{S}_i = \bar{S}_i(x)$, which are shown in Fig. 7. We note that the adjusted second nilpotent

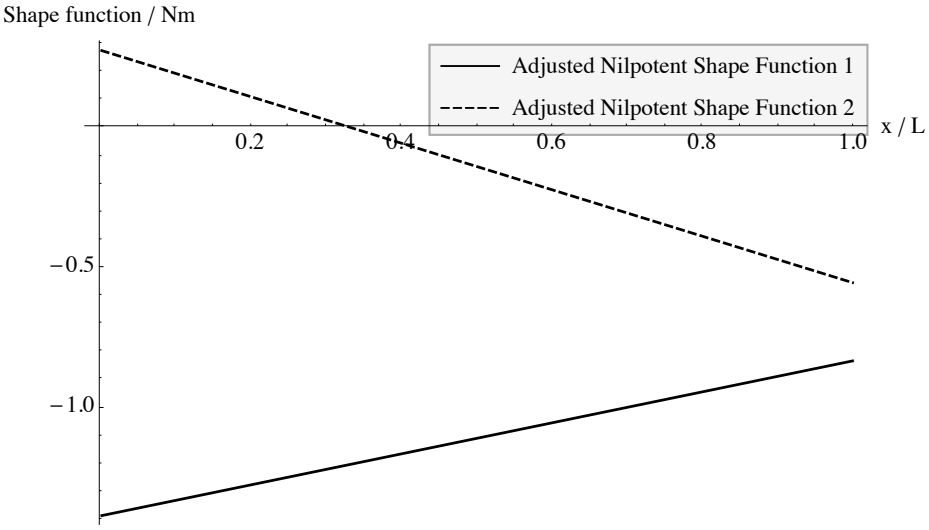

Figure 7. Adjusted nilpotent shape functions

shape function, which results from the transformation with the eigenvector belonging to the zero eigenvalue, hence from the null space of the matrix $\mathbf{A}$, has a zero value at the location of the intermediate hinge, which represents the damage in our case. Therefore, we have found the location of the damage at $x = L/3$ as the location of the zero value of the adjusted nilpotent shape function.

5.1.3 Damage quantification

To quantify the damage, we use the signals from the adjusted nilpotent sensors. For that sake the above transformation is also applied to the signals from the nilpotent sensors $y_i = y_i(\omega)$ resulting into adjusted sensor signals $\bar{y}_i = \bar{y}_i(\omega)$, which are shown in Fig. 8. Clearly, the signal from the second adjusted nilpotent sensor, which results from the transformation with the eigenvector belonging to the zero eigenvalue is trivial; hence, this sensor is nilpotent for the damaged beam. This fact has also been used to locate the damage. Yet, the signal from the first adjusted nilpotent sensor is not zero; but, it is similar to the kink at the location of the damage by means of a constant factor. Hence, this adjusted nilpotent sensor measures the kink, or, in other words the ammount of damage. This follows from the fact that the damage in this example is modelled as a hinge with a residual stiffness. Instead of using such a model, we can

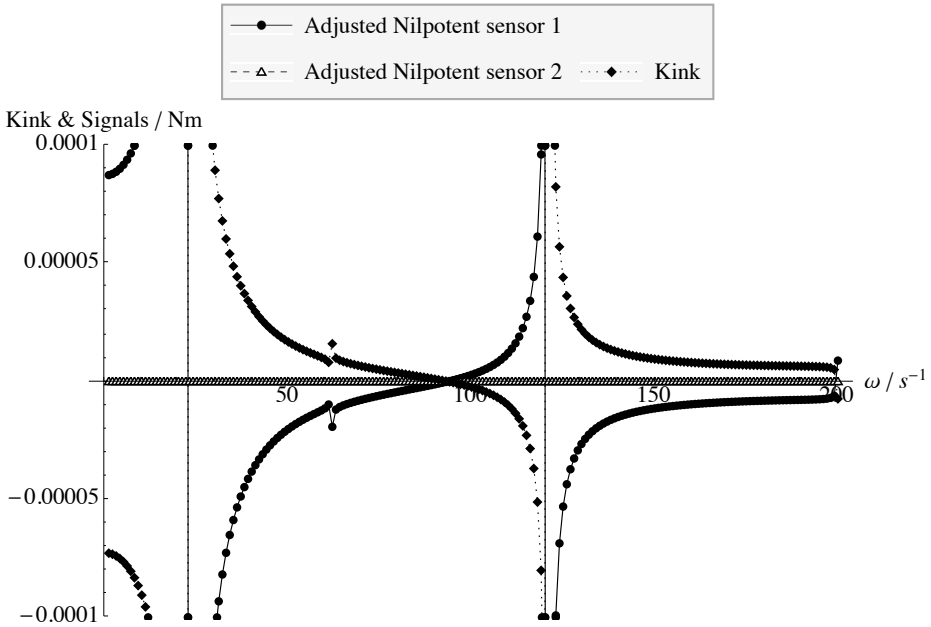

Figure 8. Adjusted nilpotent sensor signals & kink

also simulate the undamaged beam under a certain loading and account for damage by means of a local eigenstrain, whose intensity is to be determined such that the response is the one of the damaged beam. To further clarify this idea, we note that the bending moment is

$$M_y = -D\left(\frac{\partial^2 w}{\partial x^2} - \kappa_i\right). \tag{20}$$

Here, the inelastic curvature κ_i takes the role of the local eigenstrain, which is applied with an unknown intensity κ, $\kappa_i = \kappa\delta(x - \bar{x})$ at the already identified location of the damage $\bar{x} = L/3$. We can now simulate the response due to a given loading and the unknown local eigenstrain. In the harmonic case, the latter is a function of the frequency, $\kappa = \kappa(\omega)$. For the simulation, we split the beam into two parts, left and right from the location of the damage and account for the interface condition

$$[\![\frac{\partial w}{\partial x}]\!]_{\bar{x}} = \kappa. \tag{21}$$

Hence, the unknown eigenstrain intensity $\kappa = \kappa(\omega)$, which is a measure to quantify the damage, represents nothing else than the kink, which is proportional to the signal of the second adjusted nilpotent sensor from the original damaged structure. Therefore, we suggest the following strategy to quantify the damage.

1. We assume the damage has been detected and localized.

2. The signal from the adjusted nilpotent sensor, which is not trivial, has been measured under a prescribed force loading; the signal is denoted as $\bar{y} = \bar{y}(\omega)$. E.g. the signal from the first adjusted nilpotent sensor in Fig. 8 is such a signal.

3. The damaged beam is simulated as an undamged beam under the same prescribed force loading, but with an additional local inelastic curvature $\kappa_i = \kappa\delta(x - \bar{x})$, for which the signal is used in the sense $\kappa = \kappa(\omega) = \alpha\bar{y}(\omega)$. The unknown factor α is identified from the condition that the simulated signal $\tilde{y} = \tilde{y}(\omega)$ from the adjusted nilpotent sensor is identical to the measured signal.

4. Once the factor α is identified, the damage in terms of the local inelastic curvature $\kappa_i = \kappa\delta(x - \bar{x})$ is known, and the intensity $\kappa = \kappa(\omega)$ quantifies the damage.

Running through this procedure with our example problem, we identify the factor of prortionality as $\alpha = -1.20185$ and the intensity $\kappa = \kappa(\omega)$ as the kink in the damaged beam, which is also shown in Fig. 8. Clearly, such a way of quantifying damage is questionable, as it depends on the actual type of loading that is used for the procedure. However, we can further identify the actual residual stiffness of the hinge. For that sake, we compute the bending moment at the location of the hinge in the simulation, see Fig. 9, and compute the residual stiffness as the ratio between this bending moment and the intensity $\kappa = \kappa(\omega)$ of the local inelastic curvature $\kappa_i = \kappa\delta(x - \bar{x})$. In our example problem we obtain exactly the original value for the stiffness,

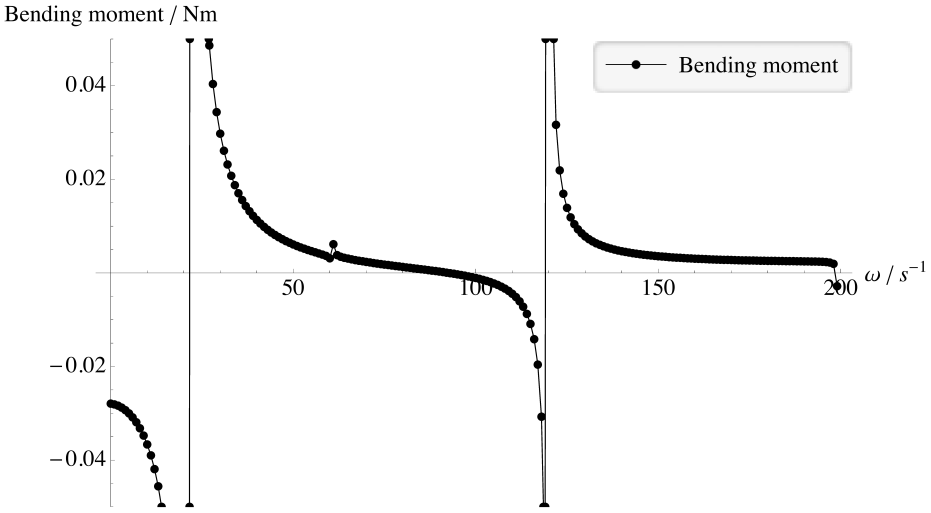

Figure 9. Simulated bending moment

$K = 383.684$.

5.1.4 Summary and discussion

Within this subsection we have shown the application of spatial compatibility filters for Structural Health Monitoring of a simple beam. The spatial compatibility filters were put into practice by means of nilpotent sensors, which are based on nilpotent sensor shape functions. The latter are statically admissible bending moment distributions for the case no external forces are applied. They exist in redundant beams only and their number is identical to the garde of

redundancy. As long as the beam is undamaged the nilpotent sensors render a trivial signal. This changes, if damage occurs; in particular, damage, which may be characterized by means of local incompatibility. From the non trivial signals in the damaged case, we can detect, localize and quantify the damage. As a specific case a damage was introduced as an intermediate hinge with a residual rotational stiffness. For this problem, we have used the simulated signals to detect the damage by introducing damage indices, to localize the location of the hinge by a proper transformation of the signals with a transformation matrix constructed from the measurements and quantified the damage by using the measurement data, which is directly related to the kink at the location of the hinge.

5.2 Generalization of the method

We complete this paper by shortly presenting a sketch on the possible extension of the method we have developed for the specific example of a simple beam to 3D problems, for which the displacement is discontinuous at an internal surface S_{12}; see Fig. 3. The first step in the method is to compute the nilpotent shape tensors from

$$\begin{aligned} V: &\quad \nabla \cdot \mathbf{S}_i = \mathbf{0}, \\ \partial V_\sigma: &\quad \mathbf{S}_i \cdot \mathbf{n} = \mathbf{0}, \end{aligned} \tag{22}$$

and put the compatibility filters with the signals

$$y_i(t) = \int_V \mathbf{S}_i \cdot\cdot\, \boldsymbol{\varepsilon} dV \tag{23}$$

into practice. We note that infinitely many nilpotent shape tensors $\mathbf{S}_i$ exist; hence, infinitely many compatibility filters are put into practice. Concerning the idea of damage detection, localisation and quantification using these compatibility filters, we note the following:

- *Damage detection* For the undamaged case none of the signals are non trivial. This changes once damage occurs; e.g. for the discontinuous displacements we have

$$y_i(t) = \int_V \mathbf{S}_i \cdot\cdot\, \boldsymbol{\varepsilon} dV = -\int_{S_{12}} (\mathbf{S}_i \cdot \mathbf{n}_{12}) \cdot [\![\mathbf{u}]\!]\, dS \neq 0, \tag{24}$$

  from which we conclude on the presence of damage; hence, we detect the damage from the fact that the signals of the compatibility filters are not trivial.

- *Damage localisation* First we note that even for the damaged case with discontinuous displacements at S_{12} nilpotent shape tensors exist; the latter may be computed from

$$\begin{aligned} V: &\quad \nabla \cdot \bar{\mathbf{S}}_i = \mathbf{0}, \\ \partial V_\sigma: &\quad \bar{\mathbf{S}}_i \cdot \mathbf{n} = \mathbf{0} \quad \text{and} \quad S_{12}: \quad \bar{\mathbf{S}}_i \cdot \mathbf{n}_{12} = \mathbf{0}. \end{aligned} \tag{25}$$

Obviously, any shape tensor $\bar{\mathbf{S}}_i$ is also a shape tensor $\mathbf{S}_i$; hence, all $\bar{\mathbf{S}}_i$ can be represented as a linear combination of the $\mathbf{S}_i$,

$$\bar{\mathbf{S}}_i = \sum_{j=1}^{\infty} \alpha_{i,j} \mathbf{S}_j. \tag{26}$$

Our method allows to compute the coefficients $\alpha_{i,j}$ from the non-trivial signals $y_i(t)$ measured in the damaged case. For that sake we introduce an inner product of two signals, which we write as $A_{ij} = \langle y_i(t) y_j(t) \rangle$; then, the inner products are used to form a theoretically infinite-dimensional matrix $\mathbf{A}$. Next, we solve the eigenvalue problem and we use the components of the eigenvectors $\mathbf{e}_i$ with corresponding zero eigenvalues $\lambda_i = 0$ as the coefficients $\alpha_{i,j}$. Once the shape tensors $\bar{\mathbf{S}}_i$ are known, the location of the damage, or better of the internal surface S_{12} is found from the fact that

$$\bar{\mathbf{S}}_i \cdot \mathbf{n}_{12} = \mathbf{0} \tag{27}$$

must hold at S_{12} for all $\bar{\mathbf{S}}_i$.

- *Damage quantification* To quantify the damage we use sensors put into practice by those sensor shape functions, which are defined as

$$\tilde{\mathbf{S}}_i = \sum_{j=1}^{\infty} \alpha_{i,j} \mathbf{S}_j, \tag{28}$$

and for which the coefficients $\alpha_{i,j}$ are obtained from the components of the eigenvectors $\mathbf{e}_i$ with non zero eigenvalues $\lambda_i \neq 0$. The corresponding signals $\tilde{y}_i(t)$ are not trivial for the damaged case. Then, we simulate the damaged case in the following sense:

1. An unknown distribution of eigenstrains $\boldsymbol{\varepsilon}^*$ is applied at the location of the damage S_{12}, which has already been found from the localisation of damage.
2. In addition external forces are used in this simulation, which are identical to the forces in the actual damaged problem, from which the signals $\tilde{y}_i(t)$ were obtained.
3. These signals are also computed in the simulation and denoted as $\hat{y}_i(t)$; they depend on the unknown distribution of eigenstrains $\boldsymbol{\varepsilon}^*$.
4. We compute the error signal $e_i(t) = \tilde{y}_i(t) - \hat{y}_i(t)$ and minimize it, from which the unknown distribution of eigenstrains is obtained.

Finally, the distribution of eigenstrains $\boldsymbol{\varepsilon}^*$ serves as a measure quantifying the damage.

Note that the discussion of the extension of the method to 3D problems was only meant to give the general idea on how to use compatbility filters for damage detection, localisation and quantification; hence, it is far from being exhaustive and from being directly applicable for practical problems at this time. Example problems for a proof of concept are planned for the future.

6. Conclusion

In the present paper we have presented the theoretical foundation of a novel method for the detection, localisation and quatification of local damage; namely *Spatial Compatibility Filters*. These filters filter the incompatible part of the strain tensor, or in other words the damage, which is closely related to the fundamental concept of incompatibility. The method can be used for damage detection, damage localisation and damage quantification. This has been validated for the simple example of a beam and an outlook on the possible extension to 3D problems has been given.

Acknowledgment

We acknowledge the support of this work from the Linz Center of Mechatronics GmbH in the framework of the COMET-K2 programme.

References

[1] C.-K. Lee and F.C. Moon, "Modal Sensors/Actuators", *Journal of Applied Mechanics* **57**(2), pp. 434-441, 1990.

[2] M. Krommer and H. Irschik, "Sensor and Actuator Design for Displacement Control of Continuous Systems", *Smart Structures and Systems* **3**(2), pp. 147-172, 2007.

[3] A. Preumont, A. Francois, P. De Man, N. Loix and K. Henrioulle, "Distributed sensors with piezoelectric films in design of spatial filters for structural control", *Journal of Sound and Vibration* **282**, pp. 701-712, 2005.

[4] A. Preumont, A. Francois, P. De Man and V. Piefort, "Spatial filters in structural control", *Journal of Sound and Vibration* **265**, pp. 61-79, 2003.

[5] A. Deraemaeker and A. Preumont, "Vibration based damage detection using large array sensors and spatial filters", *Mechanical Systems and Signal Processing* **20**, pp. 1615-1630, 2006.

[6] H. Irschik, M. Krommer and Yu. Vetyukov, "On the Use of Piezoelectric Sensors in Structural Mechanics: Some Novel Strategies", *Sensors* **10**, pp. 5626-5641, 2010.

[7] H. Irschik, M. Krommer, A.K. Belyaev and K. Schlacher, "Shaping of Piezoelectric Sensors/Actuators for Vibrations of Slender Beams: Coupled Theory and Inappropriate Shape Functions", *Journal of Intelligent Materials Systems and Structures* **9**, pp. 546-554, 1998.

[8] S.J. Wildy, A.G. Kotousov and J.D. Codrington, "A new passive defect detection technique based on the principle of strain compatibility", *Smart Materials and Structures* **17**, 045004-8pp, 2008.

[9] T. Mura, *Micromechanics of defects in solids*, 2nd ed., Springer 1987.

[10] M. Krommer, M. Zellhofer and K.-H. Heilbrunner, "Strain-type sensor networks for structural monitoring of beam-type structures", *Journal of Intelligent Material Systems & Structures* **20**, pp. 1875-1888, 2009.

[11] M. Krommer and M. Zellhofer, "Design of piezoelectric sensor networks for structural monitoring of frame structures", In: *CD-Rom Proc. of COMPDYN 2009 - ECCOMAS Thematic Conference on Computational Methods in Structural Dynamics and Earthquake Engineering*, June 30th - July 4th, 2009, Rhodes, Greece, M. Papadrakakis, N.D. Lagaros, M. Fragiadakis (eds.), 2009.

[12] M.E. Gurtin, "The Linear Theory of Elasticity", In: *Encyclopedia of Physics, Volume VIa/2, Mechanics of Solids II*, S. Flügge (ed.), Springer 1972.

[13] W. Prager and P.G. Hodge, *Theory of Perfectly Plastic Solids*, Wiley 1951.

[14] W.M. Ostachowicz, C. Krawczuk, "Analysis of the effect of cracks on the natural frequencies of a cantilever beam", *Journal of Sound and Vibration* **150**(2), pp. 191-201, 1991.